VOLTAGE STABILITY ANALYSIS USING A MODIFIED CONTINUATION LOAD FLOW AND OPTIMAL CAPACITOR BANK PLACEMENT

C. M. Muriithi, L. M. Ngoo, G. N. Nyakoe and S. N. Njoroge
Department of Electrical and Electronics Engineering, Jomo Kenyatta University of Agriculture and Technology, Kenya
E-mail: cmmuriithi@eng.jkuat.ac.ke

Abstract
This paper addresses the rising problem of identifying the voltage stability limits of load buses in a power system and how to optimally place capacitor banks for voltage stability improvement. This paper uses the concept of the continuation power flow analysis used in voltage stability analysis. It uses the modified continuation load flow to plot the PV curves of a load bus with an aggregate induction motor load. Neuro-fuzzy techniques have been used to model the induction motor load which represents an industrial load. In the subsequent predictor-corrector stages, the induction motors are increased to depict increment in loading. Different motor ratings are used in the investigations. The process starts at some base values of the system and leading to the critical point. Further the reduced Jacobian is used to strategically locate the capacitor banks in the power system so as to effect maximum voltage improvement. In case study, illustrative examples with the IEEE 30 bus system are shown. The results indicate that the modified continuation load flow captures the active and reactive power consumption of the induction motors revealing cases which could lead to voltage instability. In general, the larger rated aggregated induction motors posed a greater voltage instability risk by demanding more reactive power at lower voltages compared the equivalent lower rated aggregated induction motors. In all, manipulation of the reduced Jacobian identified the optimal placement of capacitor banks for voltage stability improvement.

Key words: Continuation load flow, induction motors, voltage stability, neuro-fuzzy

1.0   Introduction

Modern power systems are becoming more complex and heavily loaded. The issue of voltage stability has thus raised serious concerns both in planning and operation of these systems. Moreover, a significant number of power system failures have been attributed to voltage instability (Kundur; 1994). Thus, it is becoming more and more important to develop Voltage Stability Analysis tools in our current Energy Management Systems. (Sivaramakrishnan *et al,* 2009)

The determination of the security margin is a key problem to be solved in voltage stability analysis. Closely related to this is the load model used in the analysis. It has been a common practice to use static loads, but for better estimation of security margins more accurate load models are being researched. It is revealed in (Ricardo *et al* 2002) that modeling industrial loads as motors allows better analysis of the system behavior and improves the ability to reveal voltage stability problems. In (Muriithi *et al.,* 2009), the conventional load flow algorithm has been modified to incorporate a neuro fuzzy model of an induction motor load (IM), which updates the reactive power and slip during each iteration. In this modification the reactive power of the IM load which is a function of its voltage is accurately estimated, which is not the case in the conventional load flow solution (Sadaat, 2002). This model is incorporated in the modified continuation load flow.
In the present power systems, it is a common to use capacitor banks for reactive power compensation in order to sustain continuous power system reliability. However, the use of these components is very expensive, much more for developing nations which face a myriad of other power system challenges. It is therefore paramount to strategically place capacitor banks in buses that will effect the greatest improvement it the overall voltage profile. In (Kundur, 1994) the reduced Jacobian is derived for V-Q sensitivity analysis. The continuation load flow using static load models and a simple manipulation of the reduced Jacobian has been used to determine the suitable bus for capacitor placement over a range of operating points. (Sivaramakrishnan *et al.,* 2009)

This paper demonstrates how the neuro-fuzzy model of the induction motor can be incorporated in the continuation load flow. Further, different induction motor ratings are used to plot the PV and QV curves. The results indicate that though the PV curves have almost similar maximum loading, the QV curves are different for various motor ratings. This is because large induction motors consume less reactive power at base values, but as loading continues, the consumption increases drastically leading to stressed buses in terms of voltage stability. During the continuation power flow, the buses evaluated as optimal for capacitor placement are determined.

The paper is organised as follows. Section 1 served as an Introduction. In section 2, we discuss the Mathematical Formulation, section 3, a case study using the IEEE 30 bus system is demonstrated; section 4, we outline the conclusions.

2.0   Mathematical Formulation
2.1   The Continuation Load Flow Algorithm

The method of continuation power flow (Kundur;1994, Venkataramana; 2006) is dealt with in brief in this section. The conventional power flow equations based on the Newton-Raphson (NR) method for a particular bus *i* are reformulated to contain a load parameter λ.

   Let **F** be used to denote the whole set of equations, the problem can be expressed as

$$F(\partial,\underline{V},\lambda)=0$$
$$0 \le \lambda \le \lambda_{critical}$$ ……………………………………………………………………………… (1)

where $\underline{\delta}$ represents the vector of bus voltage angles and $\underline{V}$ represents the vector of bus voltage magnitudes.

The starting solution, also known as the base case solution, is determined from the conventional load flow solution. The subsequent solutions are sought over a range of λ. The dimension of F is $2n_1 + n_2$, where n_1 and n_2 are the number of *P-Q* and *P-V* buses respectively.

From the base case solution, subsequent solutions are obtained using a predictor-corrector scheme at different load levels. The corrector is a slightly modified NR power flow, while the predictor is discussed below.

Based on the starting solution, ($\lambda = 0$), a prediction of the next solution can be made by taking an appropriately sized step in a direction tangent to the solution path.   The first step in the predictor stage is to determine the tangent vector.   To obtain this, the derivative of both sides of the power flow equations is taken (2) and factorized (3).

$$d[F(\underline{\delta},\underline{V},\lambda)] = F_{\underline{g}}d\underline{\delta} + F_{\underline{y}}d\underline{V} + F_{\lambda}d\lambda = \underline{0}$$ ……………………………………………(2)

$$\begin{vmatrix} F_{\delta} & F_{V} & F_{\lambda} \end{vmatrix} \begin{vmatrix} d\underline{\delta} \\ d\underline{V} \\ d\lambda \end{vmatrix} = \underline{0}$$ …………………………………………………………(3)

The resulting equation (3) is simply the conventional Jacobian derived in subsequent iterations of the NR method. The only difference is that there is an additional column (F_{λ}). The right hand side of the equation is the tangent vector to be calculated. In order to obtain a unique solution for the vector tangent, an additional equation is added. This is accomplished by choosing a non-zero

magnitude for one of the components of the tangent vector, resulting in equation (4).

$$\begin{vmatrix} \underline{F}_\delta & \underline{F}_V & \underline{F}_\lambda \\ & \underline{e}_k & \end{vmatrix} |\underline{t}| = \begin{vmatrix} 0 \\ \pm 1 \end{vmatrix} \quad \dots\dots\dots\dots\dots\dots\dots\dots\dots\dots\dots\dots\dots\dots\dots\dots\dots\dots(4)$$

Where $\underline{e}_k$ is an appropriately dimensioned row vector with all elements equal to zero except the kth, which equals one. By choosing k correctly, and letting $t_k = \pm 1$ imposes a non-zero norm on the tangent vector. This guarantees that the augmented Jacobian will be non-singular at the critical point and enables the solution to be achieved over the entire range of λ. Having obtained the tangent vector, the prediction for the next solution is made in accordance with equation (5).

$$\begin{vmatrix} \underline{\delta}^* \\ \underline{V}^* \\ \lambda^* \end{vmatrix} = \begin{vmatrix} \underline{\delta} \\ \underline{V} \\ \lambda \end{vmatrix} + \sigma \begin{vmatrix} d\underline{\delta} \\ d\underline{V} \\ d\lambda \end{vmatrix} \quad \dots\dots\dots\dots\dots\dots\dots\dots\dots\dots\dots\dots\dots\dots\dots\dots\dots\dots..(5)$$

where "*" is the predicted solution for a subsequent value of λ, while σ is a scalar that designates the step size.

2.2 Incorporating The Continuation Load Flow to Neuro-Fuzzy Model of an Induction Motor Load

Having briefly load at the continuation load flow, we now consider the introduction of an induction motor load into its algorithm.

In the base case solution, the induction motor load is determined from the base scheduled active power at the *P-Q* bus with an induction motor load. Based on this power, the number of motors to be aggregated is determined by dividing the scheduled power with the horse power rating of the induction motor being investigated.

During the subsequent operating points ($\lambda \neq 0$) the motor load change is brought about by a change in the load parameter λ as per the equation (6).

$$P_{Li} = P_{i0} + \lambda (K_{Li} S_{\Delta base} \cos \psi_i) \quad \dots\dots\dots\dots\dots\dots\dots\dots\dots\dots\dots\dots\dots\dots\dots\dots(6)$$

where;

P_{Li0}, Q_{Li0} – original load at bus *i*, active and reactive respectively.

K_{Li} - multiplier to designate the rate of load change at bus *i* as λ changes.

Ψ_i - power factor angle of load change at bus i.

$S_{\Delta base}$ - a given quantity of apparent power which is chosen to provide appropriate scaling of λ.

Based on the newly updated scheduled power, the number of motors to be aggregated in the induction motor load is again determined as previously mentioned.

The motors are then aggregated using appropriate formulas well elaborated in (Pillay et al; 1997). Figure 1 shows the equivalent circuit of the aggregated induction motor load.
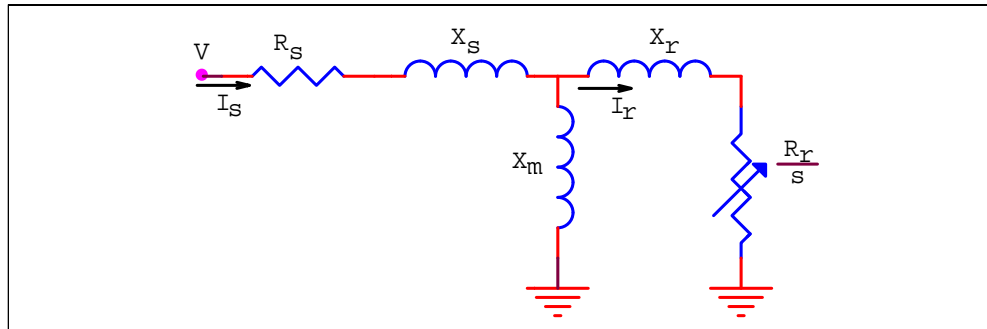

Figure 1: Per Phase equivalent circuit (squirrel-cage)

The slip curves derived at different load bus voltages for the aggregated induction motor are shown in Figure 2. Also show is the mechanical power as a function of the slip.
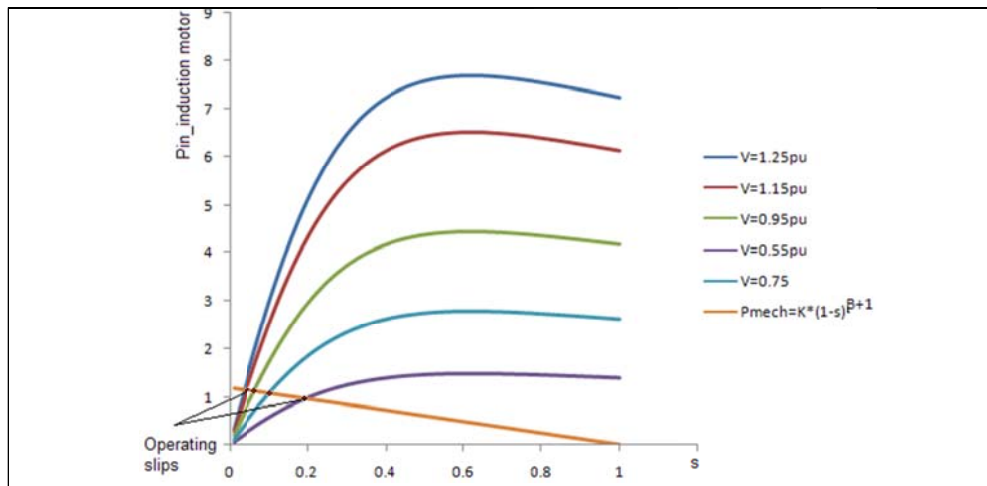

Figure 2. Electrical and Mechnical Power Slip Curves

To get neuro-fuzzy model of an induction motor load, the power balance equation (7) at the operating slips which is non-linear is solved to get the operating slip at each voltage.

$$P_{elect} - P_{mech} = 0 \quad \dots\dots\dots\dots\dots\dots\dots\dots\dots\dots\dots\dots\dots\dots\dots\dots\dots\dots\dots\dots\dots\dots\dots(7)$$

The operating slip is used to calculate the active and reactive power consumed at the load bus at each voltage . The Artificial Neuro Fuzzy Inference System is used to model the induction motor load. This is achieved by mapping the active and reactive power at operating slips to the respective voltages. The algorithm for creating the neuro-fuzzy model of the induction motor as detailed in (Muriithi et al; 2009) is summarized in Figure A1 in the appendix.

The neuro-fuzzy model of the induction motor is stored and is used to update the active and reactive powers during the iterative process of the corrector stage at each subsequent operating point.

2.3   The Reduced Jacobian Technique for Optimal Capacitor Bank Placement

The technique is carried out by a simple manipulation of the elements of the reduced Jacobian. The reduced Jacobian (Kundur; 1994) is formulated from the Jacobian of the NR load flow. A brief description of the formulation of the reduced Jacobian is given below.

The NR method aids to develop the linearized equation (8).

$$\begin{bmatrix} \Delta P \\ \Delta Q \end{bmatrix} = \begin{bmatrix} J_1 & J_2 \\ J_3 & J_4 \end{bmatrix} \begin{bmatrix} \Delta \Theta \\ \Delta V \end{bmatrix} \quad \dots \dots (8)$$

where
P and *Q* are the active and reactive power injections respectively,
V and θ are voltage magnitudes and bus angles, respectively,
Δ*P* and Δ*Q* is the active and reactive power mismatches respectively,
Δθ and Δ*V* is the change in bus angle and bus voltage magnitude respectively.

The reduced Jacobian assumes that there is no change in the active load. Thus by substituting ΔP = 0 into (8), we get

$$J_1 \Delta \Theta + J_2 \Delta V = 0 \quad \dots \dots (9)$$

$$J_3 \Delta \Theta + J_4 \Delta V = \Delta Q \quad \dots \dots (10)$$

By appropriate mathematical manipulations we get

$$\Delta Q = (J_4 - J_3 J_1^{-1} J_2) \Delta V \quad \dots \dots (11)$$

$$\Delta Q = J_R \Delta V \quad \dots \dots (12)$$

$$\Delta V = J_R^{-1} \Delta Q \quad \dots \dots (13)$$

where J_R is reduced Jacobian.

Equation (13) describes the relationship of change in the voltage magnitude Δ*V* the in terms of reactive power mismatch Δ*Q* (Sivaramakrishnan et al; 2009). In this case, Δ*Q* models a vector change in reactive power, while Δ*V* represents the resulting vector of change in the voltage magnitude.

From matrix algebra, it can be shown that the elements in each column of the inverse matrix J_R^{-1} can be made to represent the change in voltage of every load bus for a given injection of reactive power into the bus corresponding to that column (Sivaramakrishnan et al; 2009). This can be done by invoking the superposition theorem for equal reactive power injection in all the load buses. The summation of the elements of column *i* of J_R^{-1} is carried out during each stage of

the reactive power injection to a bus *i*. The sum represents the total system voltage improvement ΔV_{totali} due to the injection at the bus *i*.

The column that results in maximum ΔV_{totali} due to the injection of reactive power is deemed as the appropriate bus index to place the capacitor banks.

$$bus_i : \Delta V_{total_i} = \max \left\{ \Delta V_{total_1}, \Delta V_{total_2}, \Delta V_{total_3} \right\} \dots\dots\dots\dots\dots\dots\dots(14)$$

2.4   Case Study – IEEE 30 Bus System
2.5   System Model
We used the IEEE 30 bus system shown in Figure A2 in the Appendix, for the case study. The load bus data and line data are given in Table A1 and 2 respectively in the Appendix.

3.0   Simulation Results and Discussion
3.1   The Modified Continuation Load Flow
The continuation load flow was carried out using the IEEE 30 bus system. The algorithm was based on the equations formulated in section 2. Bus 26 was selected as the industrial load whose induction motors were increased to depict increment in loading. Based on (Pillay, 1997) the aggregate motor model and parameters were obtained from individual motors whose parameters are shown in Table A3 as found in (Franklin et al., 1997, Aree, 2006).

The number of induction motors to be aggregated was calculated from the scheduled active power at the predicted operating point at each step of the continuation load flow. Based on the aggregate motor parameters obtained, the IM load was then modeled using Artificial Neuro Fuzzy inference system as described in section 2 using the algorithm in Figure A1. The Neuro fuzzy model of the induction motor was then used in the predictor-corrector stages of the solution. This process was conducted until all the operating points were calculated.

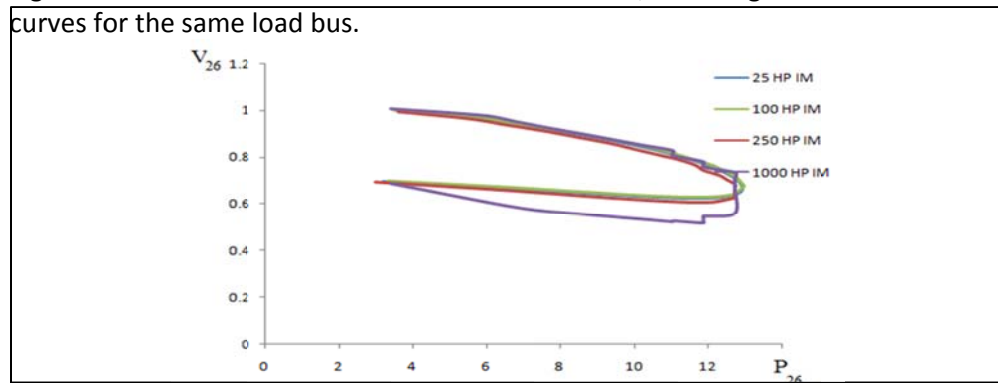Figure 3 shows the PV curves for the industrial load, while Figure 4 shows the QV curves for the same load bus.

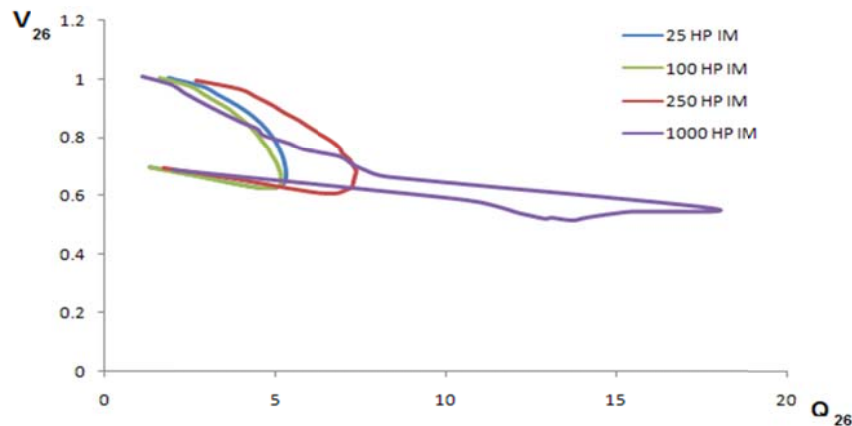*Figure 3: PV curve for bus 26 with different induction motor ratings*

Figure 4: QV curve for bus 26 with different induction motor ratings

3.2   Optimal Capacitor Bank Placement

Based on the reduced Jacobian technique the optimal bus to place a capacitor bank was determined as shown in Figure 5.
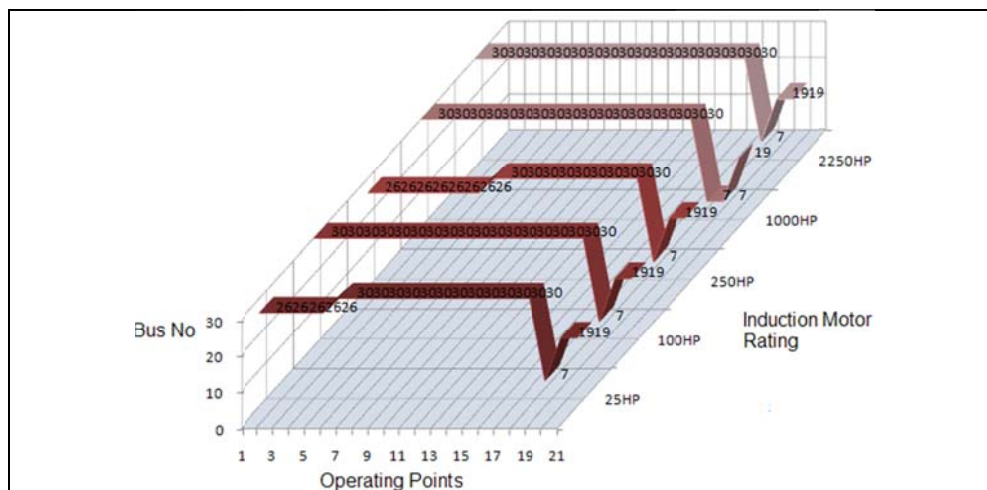

Figure 5: Optimal capacitor bank placement over operating points range

4.0   Conclusion

The modified continuation load flow with a neuro-fuzzy induction motor clearly shows that though the PV curves have almost similar maximum operating points, the QV curves are significantly different for different motors. This is because an induction motor load indicated that larger motors operate at low slips in normal rated operations, and hence consume less reactive power. But as the operating points move towards the critical loading and lower voltages, the larger motors drew more reactive power and hence posed as a greater threat to voltage stability of a system compared to their smaller counter parts. Thus depending on the induction motor ratings connected to a particular industrial load, the voltage stability risk is different.

The smoothness of the PV curve is distorted when large motors are added to depict increment in loading. This is because while in the normal continuation load flow, load increment is performed in small steps, in this modified algorithm, the increment is depicted by the individual horse power ratings of the induction motors being aggregated. Smaller increments lead to a smooth curve, while the large motor ratings are bound to distort that smoothness.

The reduced Jacobian technique successfully allocated the optimal bus for capacitor placement at each of the operating points plotted by the continuation power flow. This is important since it identifies the bus (buses) to place capacitor banks for effective voltage recovery for a particular operating point given a particular industrial load.

References

Aree P. (2006). *Load flow solution with induction motor*, Songklanakarin J. Sci. Technol., (28), **1** , pp 157-168.

Franklin D. C., Morelato A. (1994). *Improving Dynamic Aggregation of Induction Motor Models*, IEEE Transactions on Power Systems., **9**, pp. 1934-194.

Kundur P. (1994). *Power System Stability and Control*, McGraw-Hill, pp. 959-1022.

Muriithi C. M., Ngoo L. M., Nyakoe GN (2009). *Load Flow Analysis With A Neuro-Fuzzy Model Of An Induction Motor Load*, IEEE AFRICON.

Pillay P., Sabur S., M. A., Haq M. M. (1997). A Model for Induction Motor Aggregation for Power System Studies. Electrical Power Syst. Res. pp 225-228.

Ricardo M. H., Nelson M., Julio C. R. F., Antonio C. B. M., Herminio J. C. P. P and Sandoval C. Jr (2002). Impact of Induction motor Loads into Voltage Stability Margins of Large Systems –Rio Area Analysis, VIII SEPOPE.

Sadaat Hadi (2002). Power System Analysis, McGraw-Hill pp. 691.

Sivaramakrishnan R. Amit J. Ramamoorty M. Ashok V (2009). A Methodology for Selective Localization of Capacitor Banks for Power Systems, Third International Conference on Power Systems, Kharagpur, pp 318.

Venkataramana A. (2006). Lowa State University, Computational techniques for voltage stability assessment and control, Springer, pp 51-115
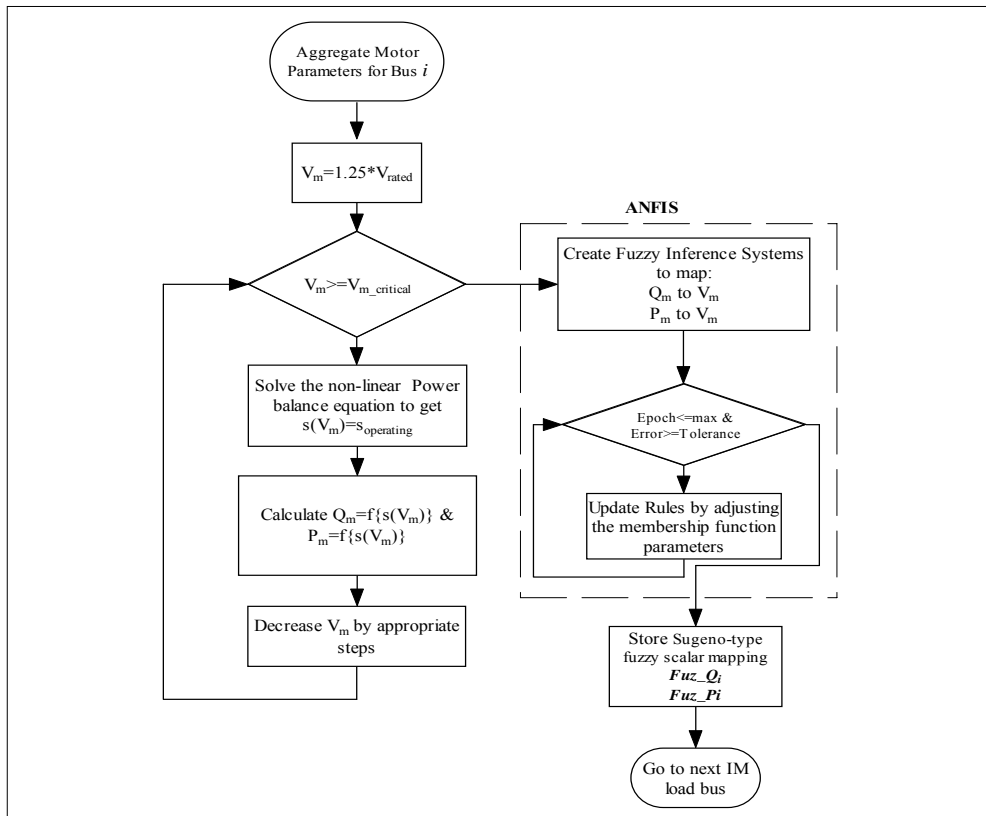
Appendix

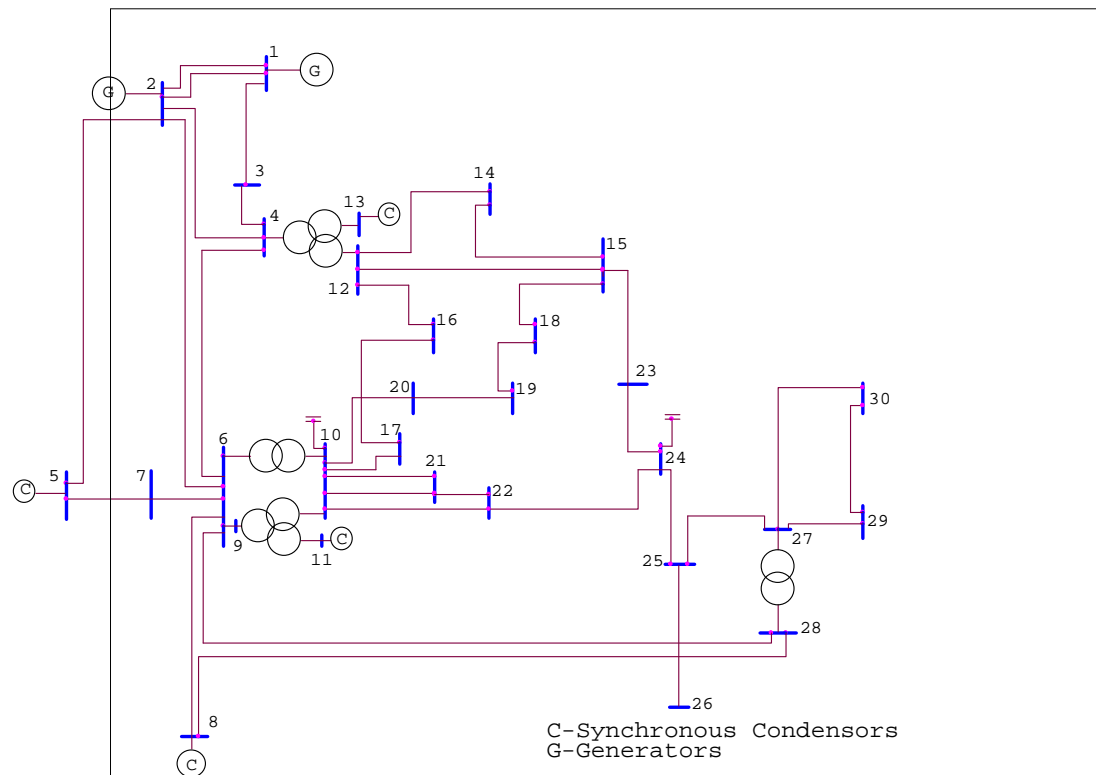*Figure A1: Algorithm for creating the neuro-fuzzy model of the induction motor*

Figure A2: IEEE 30-bus system

Table A1: IEEE 30 Bus system Load Bus Data

Bus No	Load MW	MVAr
2	21.7	12.7
3	2.4	1.2
4	7.6	1.6
5	94.2	19
7	22.8	10.9
8	30	30
10	5.8	2
12	11.2	7.5
14	6.2	1.6
15	8.2	2.5
16	3.5	1.8
17	9	5.8
18	3.2	0.9
19	9.5	3.4
20	2.2	0.7
21	17.5	11.2
23	3.2	1.6
24	8.7	6.7
26	3.5	2.3
29	2.4	0.9
30	10.6	1.9

Table A2: IEEE 30 Bus system Line Data

Bus No	Bus No	R pu	X pu	B/2 pu	Transformer tap setting
1	3	0.0452	0.1852	0.0204	1
2	4	0.057	0.1737	0.0184	1
3	4	0.0132	0.0379	0.0042	1
2	5	0.0472	0.1983	0.0209	1
2	6	0.0581	0.1763	0.0187	1
4	6	0.0119	0.0414	0.0045	1
5	7	0.046	0.116	0.0102	1
6	7	0.0267	0.082	0.0085	1

Table A2: Cont'd

Bus No	Bus No	R pu	X pu	B/2 pu	Transformer tap setting
6	8	0.012	0.042	0.0045	1
6	9	0	0.208	0	0.978
6	10	0	0.556	0	0.969
9	11	0	0.208	0	1
9	10	0	0.11	0	1
4	12	0	0.256	0	0.932
12	13	0	0.14	0	1
12	14	0.1231	0.2559	0	1
12	15	0.0662	0.1304	0	1
12	16	0.0945	0.1987	0	1
15	18	0.1073	0.2185	0	1
18	19	0.0639	0.1292	0	1
19	20	0.034	0.068	0	1
10	20	0.0936	0.209	0	1
10	17	0.0324	0.0845	0	1
10	21	0.0348	0.0749	0	1
10	22	0.0727	0.1499	0	1
21	22	0.0116	0.0236	0	1
15	23	0.1	0.202	0	1
22	24	0.115	0.179	0	1
23	24	0.132	0.27	0	1
23	24	0.132	0.27	0	1
24	25	0.1885	0.3292	0	1
25	26	0.2544	0.38	0	1
25	27	0.1093	0.2087	0	1
28	27	0	0.396	0	0.968
27	29	0.2198	0.4153	0	1
27	30	0.3202	0.6027	0	1
27	30	0.3202	0.6027	0	1
29	30	0.2399	0.4533	0	1
8	28	0.0636	0.2	0.0214	1
6	28	0.0169	0.0599	0.065	1
14	15	0.221	0.1997	0	1
16	17	0.0824	0.1923	0	1

Table A3. Induction motor parameters based on individual Horse Powers (HP)
       (f=60Hz)

HP	Rs	Rr	Xs	Xr	Xm
25	0.0219	0.0472	0.0498	0.0498	1.9504
100	0.0109	0.0472	0.0532	0.0532	2.5121
250	0.0241	0.0141	0.0864	0.864	3.0263
1000	0.0158	0.0104	0.0851	0.0851	7.6343